

Further Evidence on New Resonances in the $\bar{K}N$ System*

M. Alston-Garnjost, R. W. Kenney, D. L. Pollard, R. R. Ross, and R. D. Tripp
Lawrence Berkeley Laboratory, University of California, Berkeley, California 94720

and

H. Nicholson
Mt. Holyoke College, South Hadley, Massachusetts 01075

and

M. Ferro-Luzzi
CERN, 1211 Geneva 23, Switzerland
(Received 14 March 1977)

Utilizing the $K^{\bar{p}}$ charge-exchange results from the previous Letter, we report an energy-dependent partial-wave analysis of all available $\bar{K}N$ data from 365 to 1320 MeV/c. The effects observed at $\Lambda\eta$ and $\Sigma^0\eta$ thresholds are well described by cusps. New values of masses and widths are found for the P_{01} and P_{11} resonances. No new narrow resonances are required.

A concentrated effort towards the understanding of the low-energy $\bar{K}N$ system was made some ten years ago both in the experimental and phenomenological domain. Most of what we presently believe about the $\bar{K}N$ system and related resonances dates back to this time. Since then there has been a largely static period of re-evaluation of the data without any major experimental effort. Recently, new experimental results of much better precision have become available, leading to the hope that the quantum numbers of the less prominent features of the $\bar{K}N$ interaction can soon be established. These are (1) high-statistics bubble-chamber experiments at the lower⁻¹ and upper⁻² momentum ends of our region of interest which serve to fix the amplitudes at both ends, (2) re-measurement of the $K^{\bar{p}}$ and $K^{\bar{d}}$ total cross sections with higher accuracy, suggesting six additional narrow structures,³ (3) new electronic measurements of the $K^{\bar{p}}$ differential cross sections,⁴ (4) the precision measurement of the total charge-exchange cross section reported in the previous Letter,⁵ and (5) preliminary results on $K^{\bar{p}}$ polarization.⁶ Gopal *et al.*⁷ have reported an energy-dependent partial-wave analysis utilizing the first two of the above new results. In this Letter, we make fits to the complete data bank, including these additional experiments, and introduce some new features into the parametrization of the amplitudes.

The basic partial-wave analysis program is an outgrowth of that used by CHS⁸ into which we have incorporated a number of sophistications deemed necessary for the elastic amplitudes in this ener-

gy region. First, single-channel unitarity is imposed in the conventional way by multiplying the background S -matrix element by the resonant S -matrix element ($S = S_B S_R$, leading to a scattering amplitude $T = T_B + S_B T_R$). Resonant amplitudes are parametrized as Breit-Wigner resonances with barrier factors (of the Glashow-Rosenfeld type) appropriate to the angular momentum state. For S -wave resonances, cusps are introduced at $\Lambda\eta$ and $\Sigma^0\eta$ thresholds to reflect the observed enhancements in these channels.^{9,10} This is done by adding a partial width for these processes to the total width in the amplitude denominator: $\Gamma_T = \Gamma + \gamma_Y p$. Here p is the momentum of the η in the center of mass (imaginary below threshold) and Γ , the width without the η channel, is a free parameter of the fit as are γ_Λ and γ_Σ . Finally, the background amplitude in each partial wave has been made explicitly unitary by parametrizing it in terms of a variable scattering length, viz., $T_B = \beta A / (1 - i\beta A)$. Here β is a centrifugal barrier factor corresponding to the partial wave and $A = a + ib^2$ is the momentum-dependent complex scattering length. We square b so that the imaginary part (representing absorption) always remains positive. For S and P waves three complex coefficients of the expansion in momentum¹¹ are generally found necessary, while for D and F waves one is adequate. The latter backgrounds are thus parametrized by constant scattering lengths, whereas S - and P -wave backgrounds assume a more flexible behavior while retaining the unitary feature.

Table I shows the various types of data used,

TABLE I. Data used in the fit.

Type of data and reference	Momentum (MeV/c)	Data points	χ^2
(1) $d\sigma/d\Omega$ (K^-p, \bar{K}^0n)			
(Ref. 1)	365-425	70	176
(Ref. 8)	436-1200	685	767
(Ref. 4)	610-943		
(Ref. 12)	862-1011		
(Ref. 2)	960-1320		
$d\sigma/d\Omega(180^\circ)$	365-1320	51	124
(Refs. 1, 2, 8, and 13)			
(2) $\sigma_T, \sigma_0, \sigma_1$			
(Ref. 1)	365-425	7	45
(Ref. 3)	436-1066	108	115
(Ref. 14)	1080-1320	21	35
(Ref. 15)			
(3) K^-p polarization			
(Ref. 6)	650-1087	132	246
(Ref. 16)	862-1174	374	376
(4) $\sigma(\bar{K}^0n)$			
(Ref. 5)	515-1065	48	111
Total		1496	1995

their sources, and their contributions to χ^2 . The fit, extending from 365 to 1320 MeV/c, is anchored at the low momentum end by high statistics data in the region of $\Lambda(1520)$. For economy in computing, the number of momenta fitted was limited to 100; as a consequence, we have merged

TABLE II. Resonance parameters.

State ^a	M (MeV)	Γ (MeV)	Elasticity ^b
S_{01} ****	1670 ± 3	34 ± 5	0.16 ± 0.03
S_{01} **	1720 ± 20	175 ± 40	0.31 ± 0.05
S_{11} ****	1781 ± 10	145 ± 20	0.33 ± 0.05
P_{01} *	1600 ± 20	388 ± 50	0.21 ± 0.03
P_{11} **	1678 ± 10	33 ± 10	0.14 ± 0.03
P_{03} ****	1909 ± 20	116 ± 20	0.31 ± 0.05
P_{13} ****	[1385]	23	0.16
D_{03} ****	1519 ± 0.5	15.5 ± 0.9	0.45 ± 0.03
D_{03} ****	1690 ± 5	51 ± 10	0.21 ± 0.03
D_{13} ****	1700 ± 20	130 ± 40	0.13 ± 0.04
D_{15} ****	1781 ± 5	120 ± 10	0.36 ± 0.03
F_{05} ****	1821 ± 5	78 ± 5	0.60 ± 0.03
F_{15} ****	1934 ± 20	132 ± 20	0.13 ± 0.05
F_{17} ****	[2030]	[180]	[0.20]
G_{07} ****	[2100]	[250]	[0.30]

^aStar attributions are those of T. G. Trippe *et al.*, Rev. Mod. Phys. 48, S1 (1976).

^bWhen significant absorptive backgrounds are present, the elasticity listed is $\eta_B \Gamma_e / \Gamma$, corresponding to the diameter of the resonant circle.

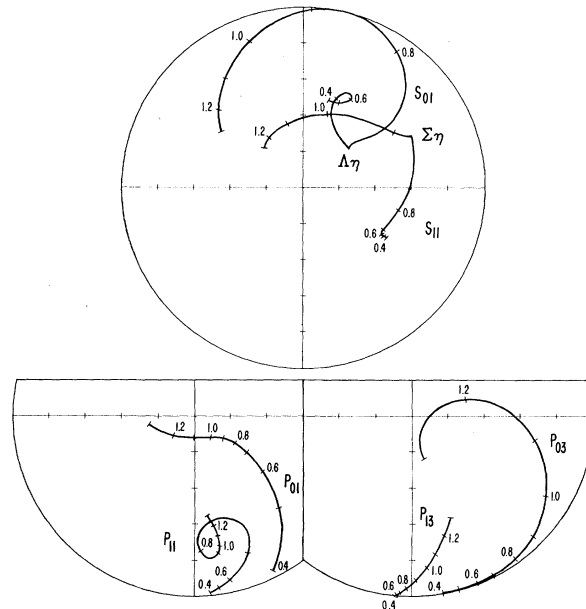


FIG. 1. Argand diagrams of the S- and P-wave amplitudes. Numbers are K^- lab momenta in GeV/c with intervals of 0.1 GeV/c indicated by bars. The S-wave cusps at $\Lambda\eta$ and $\Sigma^0\eta$ thresholds manifest themselves on the Argand diagrams as singularities in speed accompanied by discontinuities in direction.

some experiments with data points at nearby momenta. The K^-p total cross sections were interpolated to momenta where other types of data existed. Where disagreements occurred between the Brookhaven National Laboratory (BNL) total cross section measurements and those of previous experiments,^{15,17} we have chosen to use the BNL results.¹⁸ Because of these disagreements and because of uncertainties associated with deuterium corrections, the isospin-decomposed cross sections were assigned 5% uncertainty, whereas other data were introduced with their quoted statistical errors. 1496 data points were fitted, using a total of 90 parameters.

Results for the resonant amplitudes are listed in Table II. Figure 1 shows the Argand diagrams for the S and P wave amplitudes. Here we combine in each diagram the $I=0$ and 1 amplitudes to facilitate visualizing their effect on the charge-exchange cross section since the charge-exchange amplitude is the difference, $T_{\bar{K}^0n} = (T_1 - T_0)/2$. The integrated cross section, being proportional to the sum of the squares of each such amplitude, contains no interference between partial waves.

Effects of the cusps can be understood from Fig. 1. The S-wave charge-exchange amplitude,

in response to the narrow S_{01} resonance just above $\Lambda\eta$ threshold, is seen to diminish rapidly as it approaches the threshold from below. Then as the $I=0$ amplitude makes the requisite 90° left-hand turn at the cusp,¹⁹ $T_1 - T_0$ remains nearly constant immediately above threshold. This leads to a discontinuous slope in the rapidly falling \bar{K}^0n cross section as observed in Fig. 2 of the previous Letter.⁵ Similar arguments can account for the dip seen at $\Sigma\eta$ threshold, where a broader resonance in the $I=1$ amplitude occurs somewhat above this threshold. A fit with the cusps suppressed fails to follow these structures and increases the χ^2 contribution of our \bar{K}^0n data in a ± 50 MeV/c interval surrounding the cusps by more than a factor of two. An expanded view of the fits with and without cusps is exhibited in Fig. 2. Both of these S -wave resonances have been clearly seen as η threshold enhancements, and are related through SU(3) to the well-known $N\eta$ resonance. We find additionally that the S_{01} amplitude has (as does the analogous $\pi N S_{11}$ amplitude) a broader resonance at higher energy, overlapping the narrow resonance near η threshold. A second S_{11} resonance has also been suggested by the recent analysis of Gopal *et al.*⁷ with a mass of 1955 MeV; this is above our region of investi-

gation and is not required by us.

Since the discovery of $N(1470)$ with $J^P = \frac{1}{2}^+$, the existence of related hyperon resonance members of an SU(3) multiplet has been an open question. The P_{01} amplitude grows rapidly in the vicinity of $\Lambda(1520)$ and there have been several suggestions that it resonates shortly thereafter,^{7,20} while the P_{11} amplitude also gives indications of resonating at somewhat higher energy.^{7,20,21} We find that a very broad $P_{01}(1600)$ and a narrow $P_{11}(1677)$ make substantial improvements in our fit.²² Both of these have been seen in the work of Gopal *et al.*,⁷ albeit with different masses and widths. The P_{11} resonance lies in the intricate region from 700 to 800 MeV/c where three other amplitudes are known to resonate. Our mass of 1677 agrees well with the mass (1676 MeV) (Ref. 7) as determined by their $\Sigma\pi$ analysis, but not by their $\bar{K}N$ analysis (1738 MeV). However our width of 33 MeV is very much narrower than their width of 120 MeV.

Apart from $P_{03}(1910)$ at the upper end of our range, the $J^P = \frac{3}{2}^+$ amplitudes show no indication of resonant structure within our region of study. The conventional resonances in higher angular momentum states (D , F , and G) are either found to have parameters consistent with the currently accepted values²³ or, when outside of our energy region, have been fixed at these values.

Nearly all the momentum-dependent structures evident in the various polynomial coefficients are well reproduced by our fit, although the χ^2 per data point of 1.33 is high. This we believe to be mainly a reflection of systematic errors in the data and inconsistencies between experiments and, to a lesser extent, due to imperfections in the parametrization of the amplitudes. Our Argand amplitudes do resemble those of the analysis of Gopal *et al.*,⁷ despite a very different parametrization of background amplitudes and a substantially different body of fitted data. This shows that the phenomenological representation on Argand diagrams of the major features of the $\bar{K}N$ amplitudes in this energy region is basically correct and probably uniquely determined by the present data.

The isospin decomposition of the recent BNL total cross section measurements³ has indicated evidence for four new resonances in the $I=1$ channel and two in $I=0$, all lying between 500 and 900 MeV/c. They appear as narrow structures, quite weakly coupled to the $\bar{K}N$ channel. In the data which we fit, apart from these bumps appearing in the isospin decomposed cross sections, there

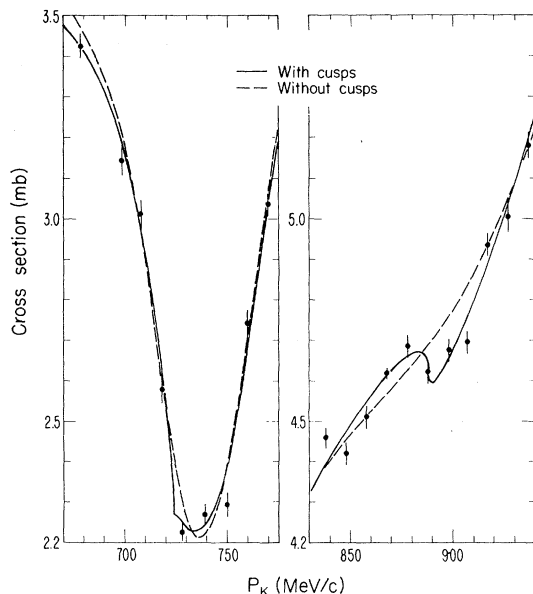


FIG. 2. Expanded view of our charge-exchange data in the vicinity of $\Lambda\eta$ and $\Sigma\eta$ thresholds showing the best overall fit obtained with and without cusps. The χ^2 coming from these data in ± 50 MeV/c intervals surrounding the thresholds is 44 with cusps and 100 without cusps; the total χ^2 without cusps increases by 101.

is no other visible indication for these resonances. To test the consistency of such resonances with other data we have selected the most prominent of the $I=1$ structures, those at 546 and 602 MeV/c. Using all data in the ± 50 MeV/c interval surrounding each one, we performed with our program a systematic exploration of possible spin-parity assignments for these resonances through D_5 . Although structure in the $I=1$ cross section was, of course, better fitted by the introduction of a resonance at the quoted mass, width, and elasticity, there was no improvement in χ^2 from any of the other data. For S and P wave assignments where the resonance may interfere with large nonresonant backgrounds of the same spin-parity, our precise charge-exchange cross sections were in fact more poorly fitted. We thus conclude that if these resonances do exist, they are most likely in the higher states (for example D_{13} as suggested by Litchfield²⁴) and can be confirmed only by a precision study of angular distributions or by investigation of other channels to which these resonances must be more strongly coupled.

We are grateful to D. Lazarus and M. Zeller for making their preliminary K^+p polarization data available for this analysis and thank R. Kelly for helpful discussion.

*Work supported by the U. S. Energy Research and Development Administration under the auspices of the Division of Physical Research.

¹T. S. Mast *et al.*, Phys. Rev. D **14**, 13 (1976).

²B. Conforto *et al.*, Nucl. Phys. **B105**, 189 (1976).

³A. S. Carroll *et al.*, Phys. Rev. Lett. **37**, 806 (1976).

⁴C. J. Adams *et al.*, Nucl. Phys. **B96**, 54 (1975).

⁵M. Alston-Garnjost *et al.*, preceding Letter [Phys.

Rev. Lett. **38**, 1003 (1977)].

⁶D. M. Lazarus and M. E. Zeller (private communication).

⁷G. P. Gopal *et al.*, Rutherford Laboratory Report No. RL 75-182 (unpublished).

⁸R. Armenteros *et al.*, Nucl. Phys. **B14**, 91 (1969), and **B8**, 233 (1968), and **B21**, 15 (1970); and B. Conforto *et al.*, Nucl. Phys. **B34**, 41 (1971).

⁹D. Berley *et al.*, Phys. Rev. Lett. **15**, 641 (1965).

¹⁰M. Jones, Nucl. Phys. **B73**, 141 (1974).

¹¹We write $a = \sum_n a_n P_n(x)$ and $b = \sum_n b_n P_n(x)$, where $P_n(x)$ are Legendre polynomials and the argument x is proportional to the momentum spanning the fitted interval, $-1 \leq x \leq +1$.

¹²M. Jones *et al.*, Nucl. Phys. **B90**, 349 (1975).

¹³P. K. Caldwell *et al.*, Phys. Rev. D **2**, 1 (1970).

¹⁴R. L. Cool *et al.*, Phys. Rev. D **1**, 1887 (1970).

¹⁵D. V. Bugg *et al.*, Phys. Rev. **168**, 1466 (1968).

¹⁶S. Andersson-Almehed *et al.*, Nucl. Phys. **B21**, 515 (1970); and M. G. Albrow *et al.*, Nucl. Phys. **B29**, 413 (1971).

¹⁷T. Bowen *et al.*, Phys. Rev. D **2**, 2599 (1970).

¹⁸The BNL data are of higher statistical precision than either Refs. 15 or 16 and tend to fall between these earlier results. However, serious disagreements often exceeding 5 mb still exist between the new experiment and its predecessors.

¹⁹See, for example, R. H. Dalitz, *Strong Interaction Physics and Strange Particles* (Oxford Univ. Press, New York, 1962).

²⁰J. K. Kim, Phys. Rev. Lett. **27**, 356 (1971).

²¹E. L. Hart, in Proceedings of the Baryon Resonance Conference, Purdue University, 20-21 April 1973 (unpublished).

²²An alternative view of an even broader P_{01} at 1700 MeV as a ninth member of the $J^P = \frac{1}{2}^+$ baryon octet has recently been suggested by M. D. Slaughter and S. Oneda, Phys. Rev. D **14**, 799 (1976).

²³There is one exception; $D_{13}(1670)$ in our analysis appears at a mass of 1700 MeV with a broader width of 131 MeV.

²⁴P. J. Litchfield, Phys. Lett. **51B**, 509 (1974).